Biophysical Journal, Volume *117*

Supplemental Information

Hydrophobic Characteristic Is Energetically Preferred for Cysteine in a Model Membrane Protein

Bharat Ramasubramanian Iyer and Radhakrishnan Mahalakshmi

SUPPORTING FIGURES

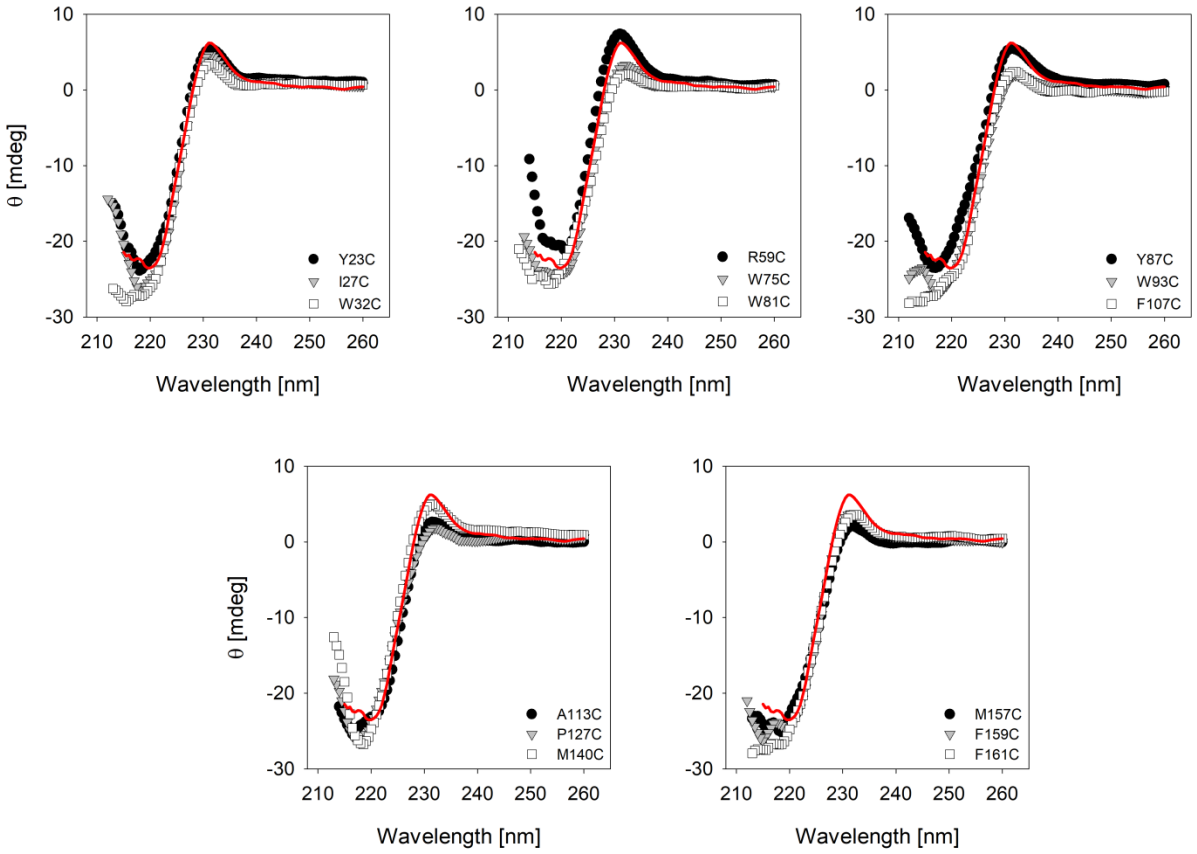

Figure S1. Secondary structure content does not vary significantly across the PagP cysteine variants. Far-UV CD wavelength scans recorded to examine the secondary structure content (negative maximum at 215 nm) and tertiary aromatic interactions attained upon barrel assembly (positive maximum at 231 nm) for a subset of PagP variants described in this study. Here, in order to exhaustively determine the folding efficiency of the mutants, we chose sufficient representatives from the midplane as well as the interface variants spanning the length of the protein. For CD measurements, 11.0 μM PagP folded in 4.0 mM DLPC SUVs was used. Shown here are raw ellipticity values (in mdeg) corrected for buffer contribution. All the PagP variants described here show similar secondary structure content (comparable θ_{215} values), indicating that they attain a similar folded state upon assembly into lipid vesicles. Minor variations in the interaction geometry of Y26 and W66 that contribute to the observed tertiary CD (1) can account for the differences observed in the θ_{231} values. However, the θ_{231} does not correlate with the stability of PagP (2). Data for wild-type PagP is shown as red spline curve in each panel.

A

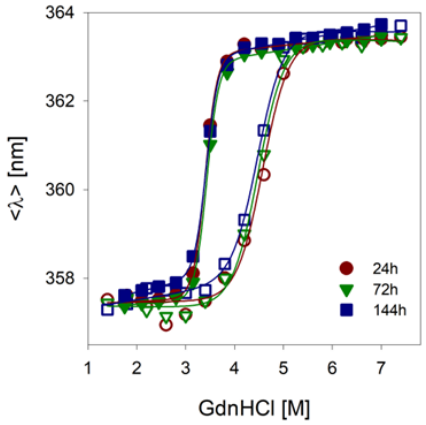

B

Time (days)	ΔG_F (kcal/mol)	ΔG_U (kcal/mol)	$C_{m,F}$ (M)	$C_{m,U}$ (M)
1	16.06	9.89	3.33	4.42
3	16.20	9.67	3.36	4.33
6	16.17	9.67	3.35	4.32

Figure S2. PagP exhibits hysteresis in DLPC vesicles at alkaline pH. (A) Overlay of folding (filled symbols) and unfolding (hollow symbols) profiles of PagP-WT derived from GdnHCl-mediated chemical denaturation. Here, we have utilized average wavelength values (<λ>) (3) as a measure of the folded population of the protein in solution. Even after prolonged incubation, we find that the folding and unfolding titrations do not converge, thereby showing hysteresis. (B) Time-course of free energy values of folding and unfolding (ΔG_F and ΔG_F, respectively) and denaturation midpoint values ($C_{m,F}$ and $C_{m,U}$, respectively) derived for folding and unfolding titrations by fitting the average wavelength data to the two-state mechanism. The folding titration profiles were fit using a global *m* value of $m = 4.83 \pm 0.19$ kcal mol^{-1} M^{-1}. For the analysis of the unfolding profiles, we used the global *m* value of $m = 2.24 \pm 0.17$ kcal mol^{-1} M^{-1}. Based on the cooperativity of the transition (*m* value) for the individual profiles, we can predict that the unfolding profile deviates from equilibrium behavior for PagP in DLPC SUVs. Such a kinetically unattained two-state system, as opposed to the path-independence reported earlier (4), could arise from the use of SUVs or the alkaline pH of 9.5 at which the measurements are done.

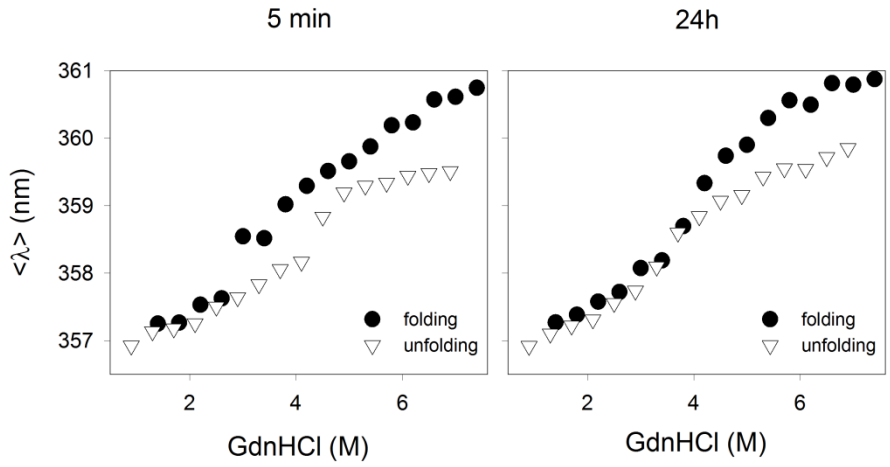

Figure S3. Equilibrium folding profiles of PagP-WT in citrate buffer pH 3.8. Representative folding (filled symbols) and unfolding (open symbols) titrations monitored using change in fluorescence emission profiles of tryptophan. We observe that the profiles do not overlap even after prolonged incubation (of up to 72 h), resulting in hysteresis, in GdnHCl-mediated denaturation. The unfolding is incomplete, as is evident from the <λ> obtained in 6.0-7.0 M GdnHCl (<λ> of 364 nm obtained in the case of pH 9.5; see Fig. S2). Further, the unfolding/ folding profiles show poor cooperativity (low *m* values) compared to what we obtain at pH 9.5, indicating the likely existence of a multistate event.

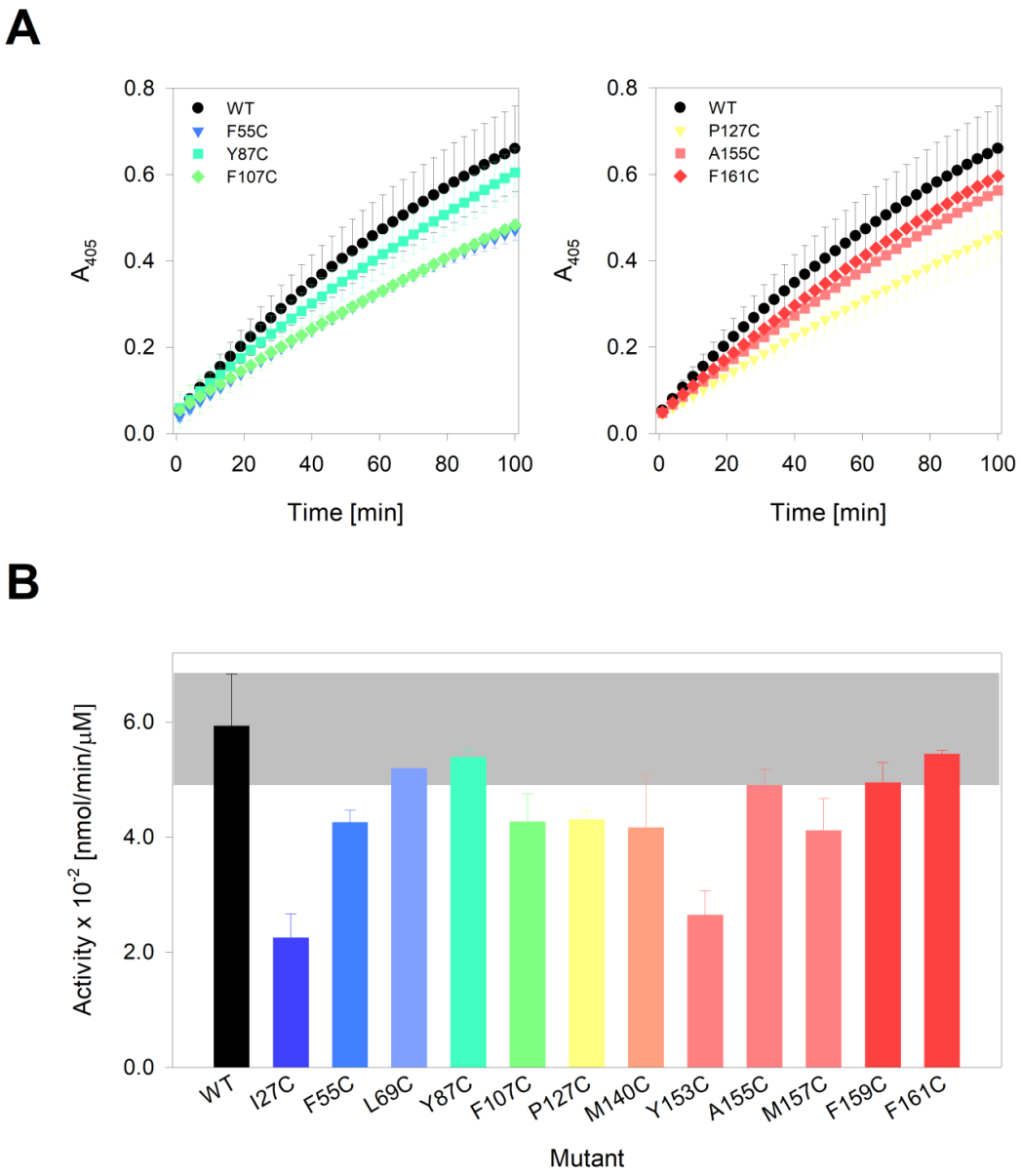

Figure S4. Lipase assay to monitor the activity of PagP cysteine variants. (A) Change in A_{405} (absorbance at 405 nm) was recorded over time as an indicator of *p*NPP hydrolysis and *p*-nitrophenol release, based on a previously reported protocol (5). Data was obtained using 1.0 µM protein folded in 1.2 mM DLPC and averaged over two independent experiments. Shown here is the data for a subset of PagP variants described in this study. Data for wild-type PagP is shown in black. A rainbow color scheme (N→C terminus) is used for the scatter plots.(B) Specific enzyme activity for each PagP variant was derived using the rate of change in A_{405} and compared with wild-type PagP. The gray bar denotes the standard error obtained for the specific activity of wild-type PagP. All cysteine variants tested for activity, except I27C and Y153C, show comparable levels of specific enzyme turnover. The reason for lowered activity in both these mutants is not clear, as this does not correlate with the measured stability of these proteins.

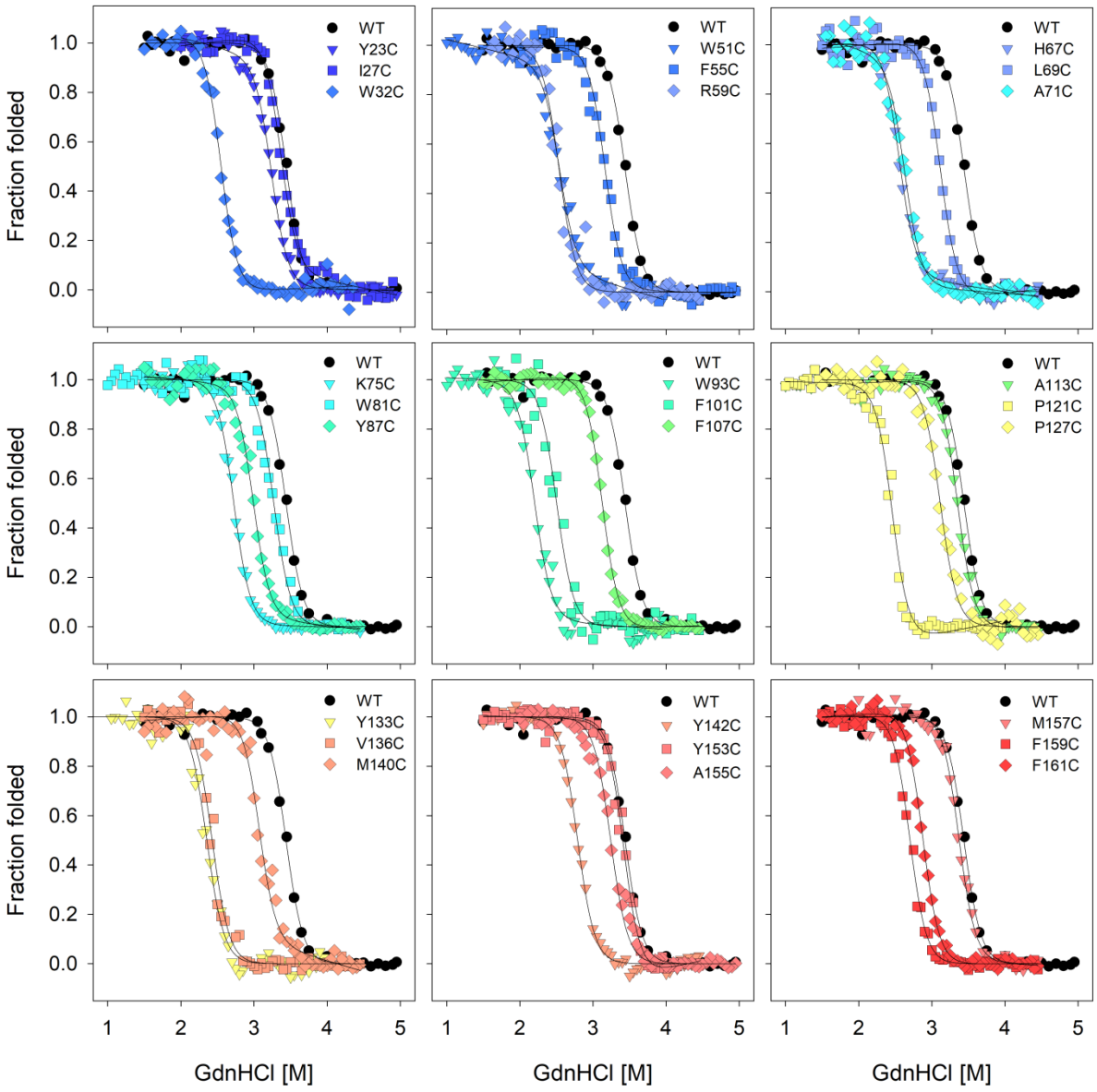

Figure S5. Equilibrium folding profiles derived for the PagP single cysteine variants. Representative folding titrations displayed as folded fraction (f_F) for all the single-cysteine containing PagP variants studied here. Scatter plots are colored in a gradient of red to blue based on the position of host site at which cysteine has been incorporated, ranging from Y23C located near the N-terminus (top left, bright blue), to F161C situated towards the C-terminus (bottom right, bright red). Folding profiles were acquired by monitoring the change in fluorescence emission intensity at a λ_{em} of 340 nm, corresponding to the $\lambda_{em\text{-}max}$ of the folded protein. Datasets were fitted to the two-state equation (3) (representative fits are shown as solid lines). Data for wild-type PagP is shown in black in each panel. -

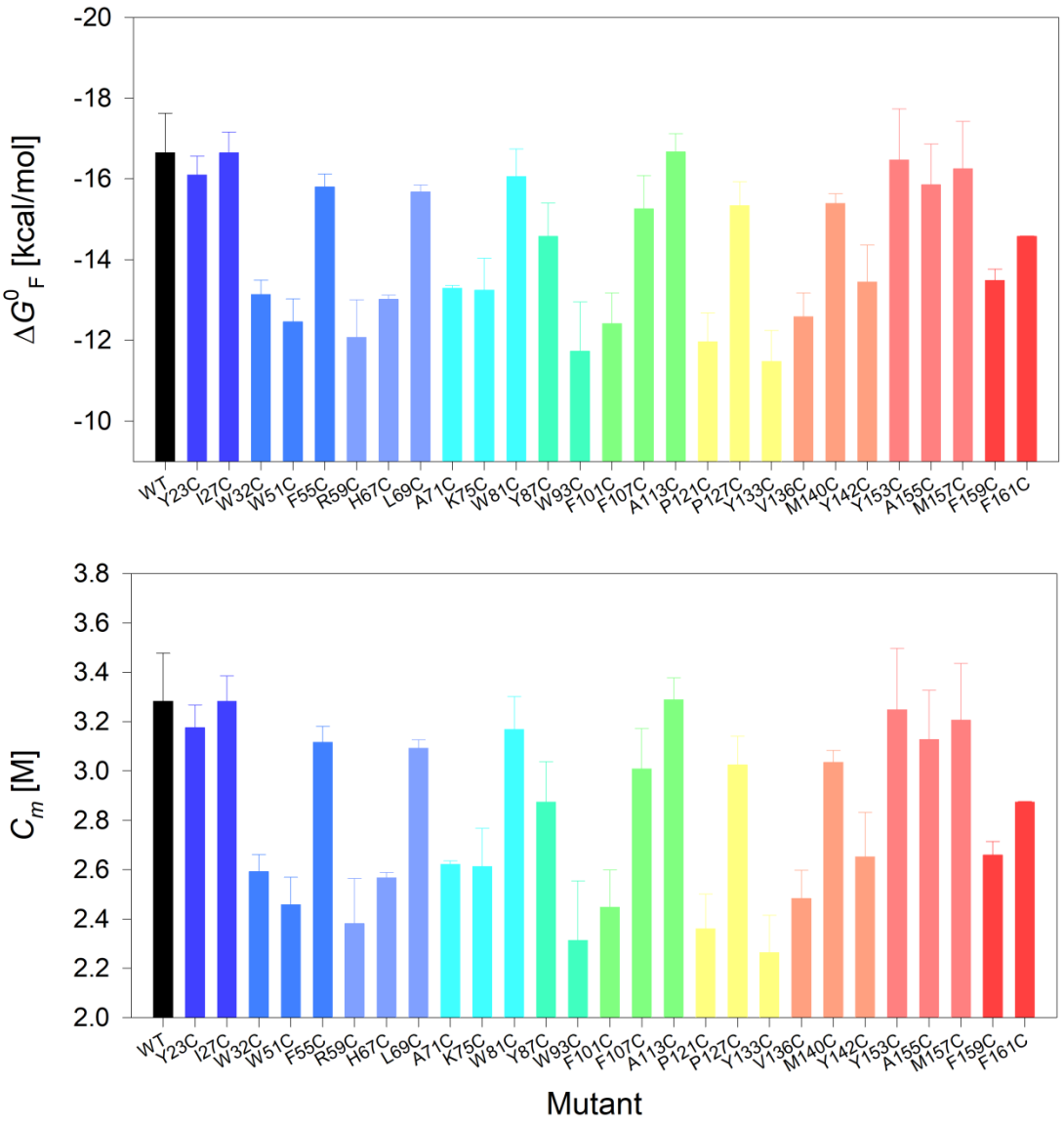

Figure S6. Equilibrium folding free energy values derived for the PagP single cysteine variants. Histograms indicating the thermodynamic parameters derived for the PagP single-Cys mutant library. The equilibrium free energy of folding (ΔG^0, upper panel) and the midpoint of chemical denaturation (C_m, lower panel) have been denoted as vertical bars against the single letter abbreviation of the particular mutant. Data is represented as mean and standard deviation from two independent experiments. The color code for the scatter plot is retained from Fig. S5. WT: wild-type PagP.

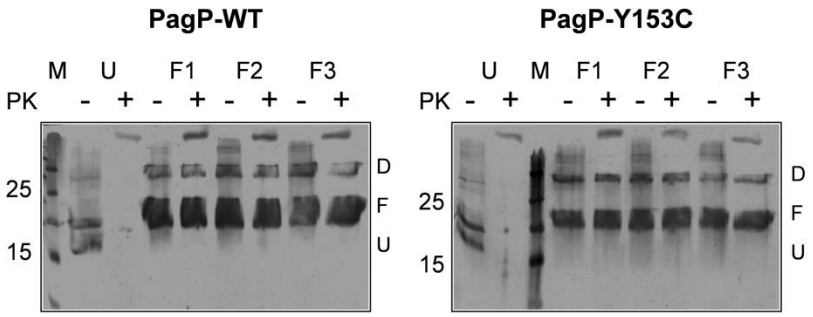

Figure S7. Folding of PagP variants monitored by electrophoretic mobility shift assay and proteolysis. Gel mobility shift and protection against proteolysis by proteinase K (PK) of PagP-WT and one representative mutant (Y153C) from the PagP cysteine mutant library was used as evidence that the PagP variants are indeed folded. Folded (F) and unfolded (U) proteins differ in their electrophoretic mobilities and only the well-folded protein shows resistance to digestion by PK. F1-F3 correspond to the first three samples in the equilibrium folding studies, and possess increasing amounts of GdnHCl in the sample (1.5 M – 1.6 M). Unfolded sample (U) is generated by adding SDS gel loading dye to folded sample (F) and thereafter, boiling it for 3 min. PagP also shows a substantial population of protein dimer (D). M: Marker (molecular weights in kDa are indicated on the left of each gel).

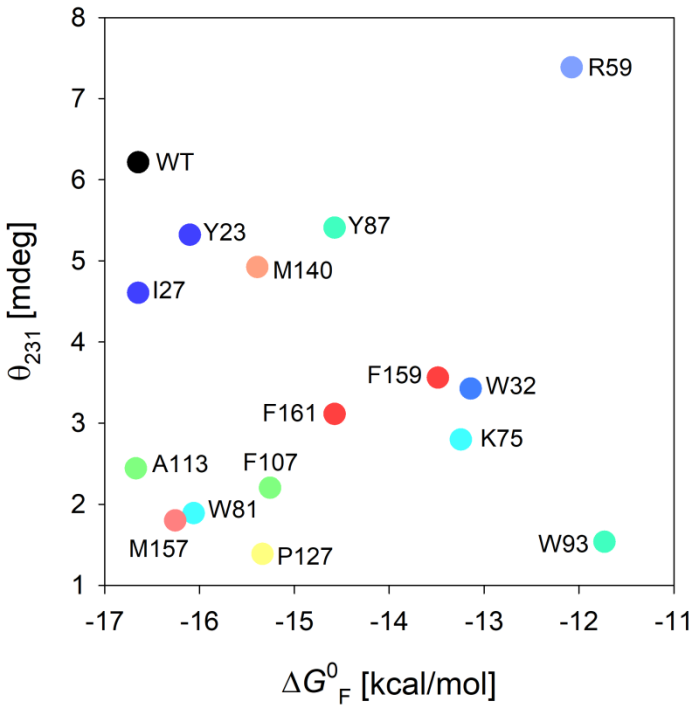

Figure S8. Correlation of the folding free energy with the tertiary interaction of the Cys mutant library. Correlation plot derived by mapping the folding free energy for a subset of single-Cys variants (X→C) with the the tertiary interaction (θ_{231} values) derived from the far-UV CD wavelength scans (Fig. S1). Here we find that the θ_{231} value, which is a reliable indicator of tertiary packing, carries reasonable variation across mutants ranging from approximately +7 mdeg (strong tertiary interaction) for PagP-R59C to approximately +2 mdeg (poor tertiary interactions) for PagP-P127C. However, a clear correlation between θ_{231} and the ΔG^0_F was not observed. Mutants are labeled using the single letter code for each amino acid followed by the residue position at which the substitution has been carried out. The color code for the scatter plots is retained from Fig. S5.

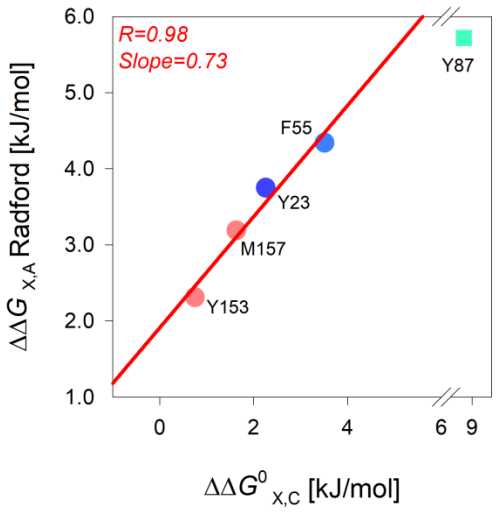

Figure S9. Correlation of the energetic cost of cysteine incorporation with reported cost of alanine substitution. Correlation plot derived by mapping the partitioning free energy for a subset of single-Cys variants (X→C) with the energetic cost of substitution to alanine (X→A) at the same host site calculated from a previous study that carried out ϕ-value analysis of PagP folded in DLPC vesicles (6). Regression coefficient for the correlation is indicated at the bottom right, and a linear fit to the correlation is shown as a solid red line. Points excluded from the fit are shown as square symbols. Mutants are labeled using the single letter code for each amino acid followed by the residue position at which the substitution has been carried out. The color code for the scatter plot is retained from Fig. S5.

SUPPORTING REFERENCES

1. Khan, M. A., C. Neale, C. Michaux, R. Pomes, G. G. Prive, R. W. Woody, and R. E. Bishop. 2007. Gauging a hydrocarbon ruler by an intrinsic exciton probe. Biochemistry 46(15):4565-4579.
2. Iyer, B. R., P. V. Vetal, H. Noordeen, P. Zadafiya, and R. Mahalakshmi. 2018. Salvaging the thermodynamic destabilization of interface histidine in transmembrane beta-barrels. Biochemistry 57(48):6669-6678.
3. Moon, C. P., and K. G. Fleming. 2011. Using tryptophan fluorescence to measure the stability of membrane proteins folded in liposomes. Methods Enzymol. 492:189-211.
4. Marx, D. C., and K. G. Fleming. 2017. Influence of Protein Scaffold on Side-Chain Transfer Free Energies. Biophys. J. 113(3):597-604.
5. Iyer, B. R., and R. Mahalakshmi. 2015. Residue-Dependent Thermodynamic Cost and Barrel Plasticity Balances Activity in the PhoPQ-Activated Enzyme PagP of Salmonella typhimurium. Biochemistry 54(37):5712-5722.
6. Huysmans, G. H., S. A. Baldwin, D. J. Brockwell, and S. E. Radford. 2010. The transition state for folding of an outer membrane protein. Proc. Natl. Acad. Sci. U. S. A. 107(9):4099-4104.